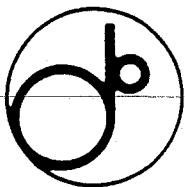


New Folder Name Slow Drift



Slow Drift and Frequency Spectra on Ground Motion

S. TAKEDA, A. AKIYAMA, K. KUDO,
H. NAKANISHI and N. YAMAMOTO

*Submitted to the Third International Workshop on Accelerator Alignment,
Annecy, France, Sept. 28 - Oct. 1, 1993.*

National Laboratory for High Energy Physics, 1993

KEK Reports are available from:

Technical Information & Library
National Laboratory for High Energy Physics
1-1 Oho, Tsukuba-shi
Ibaraki-ken, 305
JAPAN

Phone: 0298-64-1171
Telex: 3652-534 (Domestic)
(0)3652-534 (International)
Fax: 0298-64-4604
Cable: KEK OHO
E-mail: LIBRARY@JPNKEKVX (Bitnet Address)
library@kekvax.kek.jp (Internet Address)

SLOW DRIFT AND FREQUENCY SPECTRA ON GROUND MOTION

S. Takeda, A. Akiyama, K. Kudo, H. Nakanishi and N. Yamamoto
KEK, National Laboratory for High Energy Physics
Oho, Tsukuba-shi, Ibaraki-ken 305, Japan

1. INTRODUCTION

Quantitative description on ground motion has become the center of interest, in relation to the construction of large scale and high luminosity machines. Especially, general consciousness regarding vibration problems has been raised in the frequency band from 0.01 to 100 Hz [1]. Concerning noise behavior of the gravitational wave detector, a large amount of data has been accumulated in the frequency range between 0.1 Hz and 1 kHz. In summing up, the following are features. An empirical power law form of the ground-noise spectrum, except sharp peaks and/or broad peaks from the observed spectrum, can be given by $P(f) \approx kf^{-2}$, where $P(f)$ = a power spectrum in $m/\sqrt{\text{Hz}}$, k = constant and f = frequency in Hz. The factor k changes with site dependence, from 10^{-7} to 10^{-9} $m/\sqrt{\text{Hz}}$, in the frequency span ≈ 1 to 100 Hz. In the rest frequency range, k is 10^{-9} $m/\sqrt{\text{Hz}}$ [2]. Therefore, the empirical power law of ground motion in those frequency ranges is applicable to the design of an accelerator. At present time, it seems that there is not enough of the necessary basic information about the power spectrum function with the frequency band less than 1 mHz. We wish to turn to another region of a motion spectrum, namely slow drift. In the world of micron-level alignment, we will see that this problem can become fatal.

A long term drift and slow periodical fluctuations of the vertical beam position were found in the TRISTAN. During a high luminosity run, performance of the TRISTAN main ring strongly depends on the closed orbit. The very small amounts of changes of the closed orbit induce significant reduction of the maximum bunch current at the injection energy, and the specific luminosity at the colliding energy. Gradual movements of the orbit were observed without any intentional change of machine parameters [3]. The vertical r. m. s. movement of the closed orbit distortion is larger than the horizontal one. When the former grew larger than 0.1-0.2 mm, the bunch current decreased significantly, and the beam lifetime became shorter. To make the possible error sources of the vertical movement clear, a study has been made to specify the source of the phenomena [4]. Secular and local deformation of the tunnel by the ground movement, having in a frequency band much lower than the seismic one, correlated with the vertical beam fluctuations.

The next generation of linear colliders requires alignment stabilities of component placement at least two or three orders of magnitude better than can be achieved by the conventional methods. Tolerance of the final focus system for JLC-I is shown in Ref. [5]. The beam based alignment technique will play an important role to recover its proper alignment for low frequency ground motion [6]. Figure 1 shows that the tolerance for the launch offset of the incoming beam is nearly 1 σ in both directions. In other words the entire system can shift 1 μm in the vertical and 10 μm in the horizontal directions without damaging the spot size.

This report deals mainly with the slow drift of vertical ground motion at the mountainside tunnel, to get the normal power spectrum density for the frequency band less than 1 mHz. In chapter 4, however, we give an empirical spectrum law of vibration or ground motion for wide frequency bands, from 1 nHz to 100 Hz, to guess the tolerance of the machine.

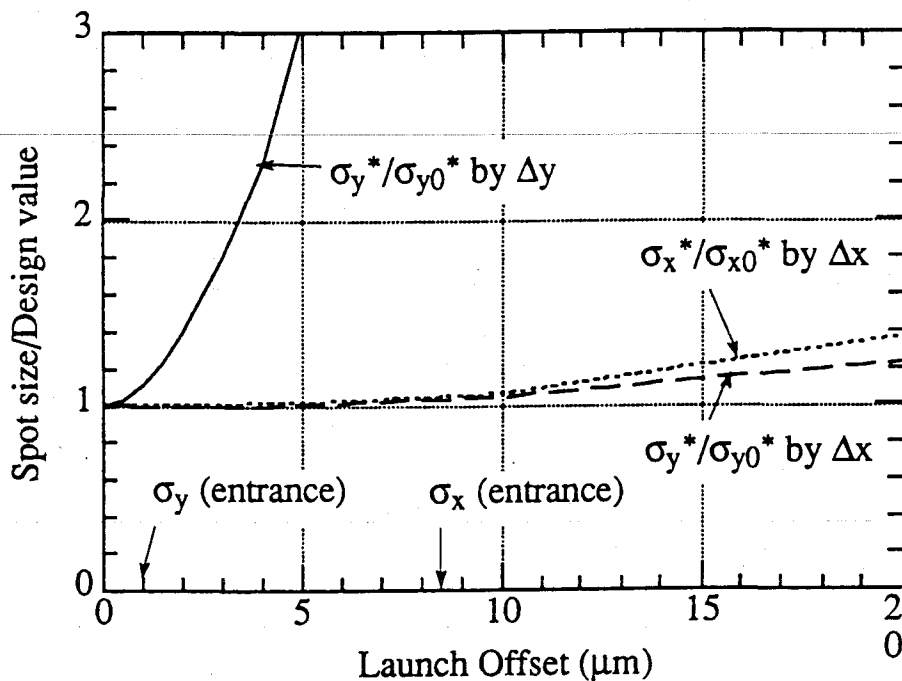


Fig. 1. The spot sizes at IP normalized by the design values as functions of the launch offset at the entrance of the final focus system.

2. INSTRUMENTS AND METHODS

Figure 2 shows a schematic description of the water-tube tiltmeter system to observe the ground motion [7]. Figure 3 shows an example of installation in the mountainside tunnel^{*)}. Two pots and a connecting tube are made with pyrex. The tiltmeter, originally developed by Ishii et al. [7], is equipped with a float without mechanical suspension and an inductive linear-sensor^{**)}. An aluminum disk having a diameter of 50 mm is mounted on top of the float. A narrow gap between the sensor and the disk is measured by inductive coupling. The tiltmeter for a long baseline is to measure the difference between the gaps of each pot. This method of tiltmeter offers several advantages. The inductive sensor integrates over the disk and vibrations on the water surface are averaged out by the large massive float. Continuous series of measurements and collection of data from remote places are also available over a long period using an automatic data-taking system.

A water-tube tiltmeter potentially brings with it a large sensitivity to temperature because of the high volumetric thermal coefficient of water, that is 2.1 $\mu\text{m}/\text{degree}/\text{cm}$. If the pot is heated up on one side, the level of the water in that pot rises while remaining unchanged in the other. Temperature sensors are also attached to the pots, and their values are used to correct the data. The output signals from sensors are sent to a computer via 16 bit A/D converter. Sampling rates of the data is 10 Hz. Total errors, in the worst case, are within accuracy of 0.1 μm . In order to connect the present data with those high frequency data, we also observed the ground motion with the broadband seismometer^{***)}.

The measurements of the vertical movement are made at the straight section of the mountainside tunnel^{*)}. A set of the tiltmeter was installed at a distance of 48 meters, as shown in Fig. 3. The straight section is located at the distance, 1 km, from the entrance of the tunnel, then the tiltmeter is not influenced very much by the temperature. Tiltmeters of the same kind have been installed in the tunnel of KEK [4].

*) Old Sazare-mine, Sumitomo Metal Mining Co., Ltd., in Shikoku, Japan.

***) IWA-30U-9001, Baumer Electric AG, Switzerland. ***) CMG-3 and STS-2.

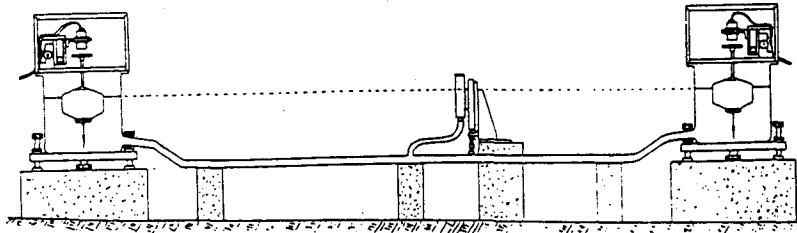
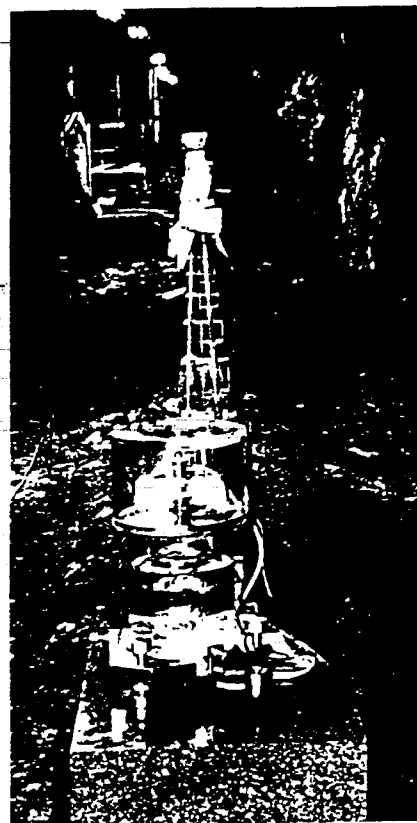


Fig. 2. Schematic description of the water-tube tiltmeter.

Fig. 3. Experimental setup for water-tube tiltmeter.



3. RESULTS AND ANALYSIS

Figure 4 shows an example of long term measurements and the results of decomposition by the computer program, BAYTAP-G [8, 9]. This program is a quite new method for tidal analysis proposed by Ishiguro [8] based on the concept of Bayesian statistical modeling, ABIC: Akaike's Bayesian Information Criterion [10]. BAYTAP-G decomposes the input data into a tidal part, a drift part, a response part and an irregular part under the assumption that the drift is smooth. The analysis model is obtained by maximizing the posterior distribution of the parameters. For the given data ABIC is used to select the optimum values of the hyperparameters of the prior distribution and combination of parameters.

Data of 35 days were analyzed using BAYTAP-G and the results are shown in Fig. 4. Each component of the tide, drift and irregular noise was estimated at every 30 minute's data point. The magnitudes of the drift and irregular part were less than $\pm 0.12 \mu\text{rad}$ and $0.01 \mu\text{rad}$ respectively for all of the data points in Fig. 4.

Atmospheric pressure is also observed simultaneously to check the meteorological effects on the ground motion. Figure 5 presents a drift obtained from BAYTAP-G and the atmospheric pressure observed at the same place. We can see in this figure that the drift roughly correlates to the atmospheric pressure. Detailed examination about the data, however, reveals that the atmospheric pressure is only an example out of the source for the drift. The changes in ground water act, in some case, as a significant cause of drift [11]. In addition, the effect of precipitation has complex features. Its affection is sometimes very large having a connection with the action of underground waters. It is not rare that the amount of drift due to precipitation of 100-200 mm reaches to the value of the order of $1 \mu\text{rad}$ [11]. Figure 6 shows a large change of the drift between 250 and 350 hours, which corresponds to a heavy rain around these days, but unfortunately, the falling of a thunderbolt cut the electric power to our system.

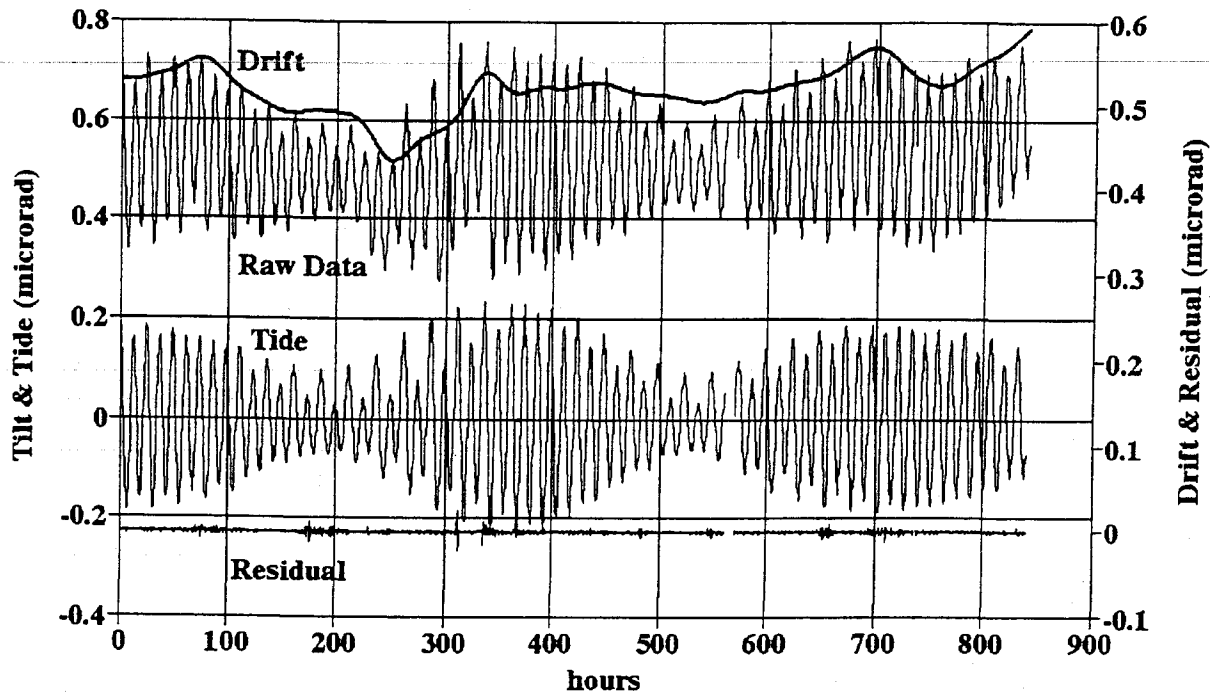


Fig. 4. A 35 day record of ground motion in the mountainside tunnel. (From 25/01/1993 to 28/02/1993).

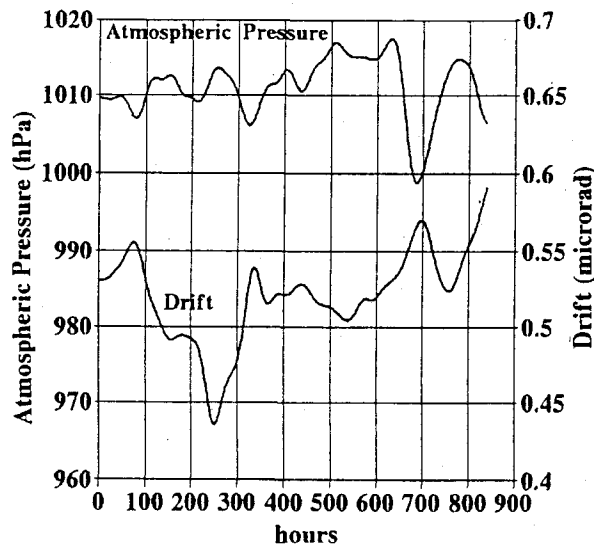


Fig. 5. Drift and atmospheric pressure. (25/01/1993-28/02/1993).

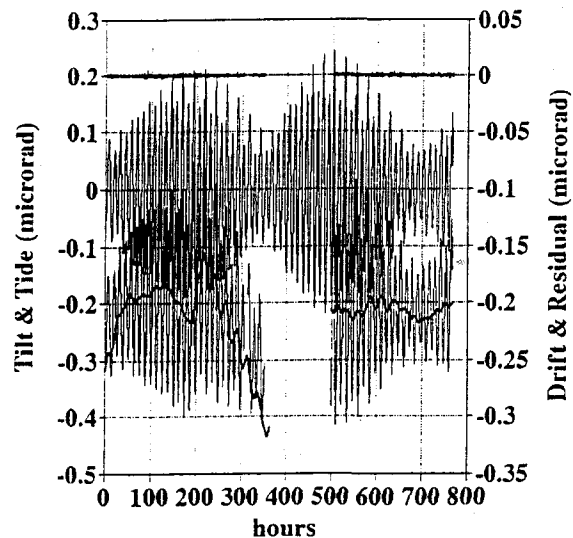


Fig. 6. Effect of precipitation. (06/10/1992-06/11/1992).

Considering from a signal processing point of view, the observed drift is an input signal to the transfer function of accelerator system, then we need only its amplitude and frequency characteristics for analyzing the system. Figure 7 shows a power spectrum observed by the tiltmeter. One can see several peaks with frequency of around 0.04 and 0.08 1/hour in Fig. 7. The origin of these peaks is the earth tide. The actual tidal signal is quite complicated in that several periods are represented for both the moon and the sun because of orbit ellipticities and inclinations etc.. Table 1 shows the major tidal periods and relative amplitudes calculated by BAYTAP-G.

Table 1
Major Periods and Relative Amplitudes

Symbol	Name	Period	Amplitude
M2	Principal lunar	12.42 h	26.91
S2	Principal solar	12.00 h	10.69
O1	Lunar declination	25.82 h	3.96
K1	Lunisolar	23.93 h	5.67

Figure 7 also shows that random components are included in the ground motion. Figure 8 shows monthly variances of the drift calculated by BAYTAP-G. Although the data points are not so many, we may say that the ground motion is described in terms of the 1/f noise rather than the white noise. In other words, the ground motion is nonstationary or time dependent.

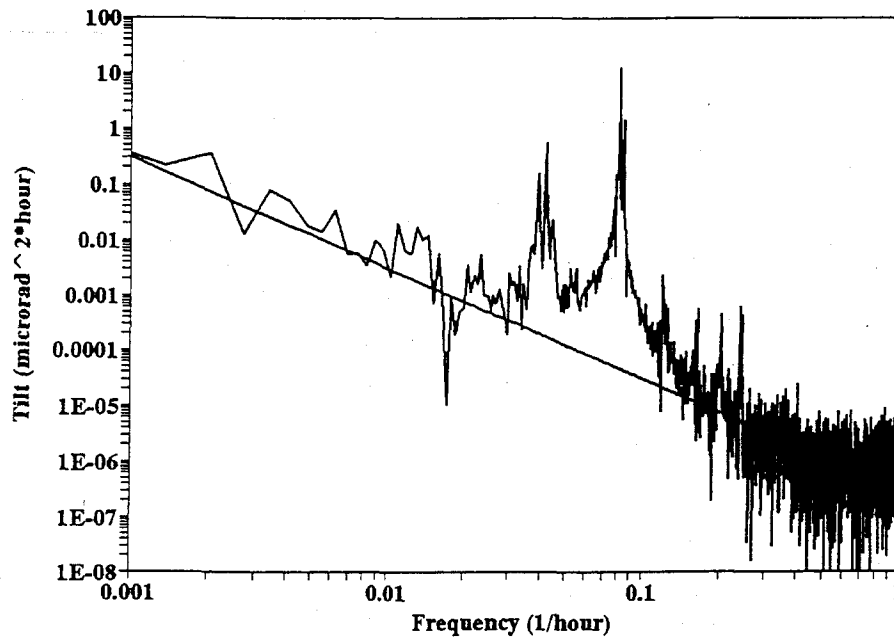


Fig. 7. A spectrum of ground motion. A straight line indicates 1/f.

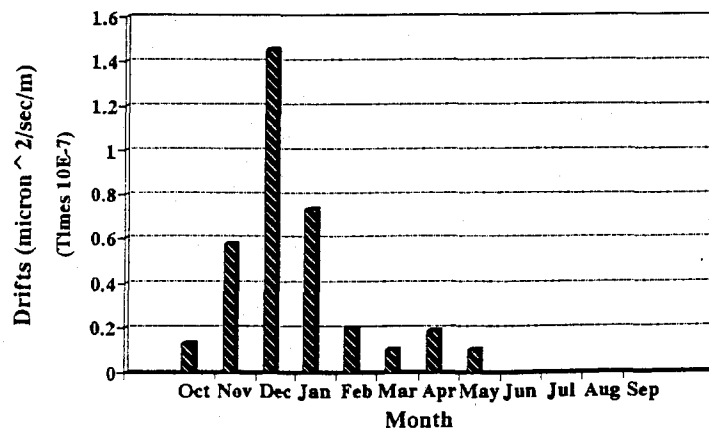


Fig. 8. Monthly variance of drifts at Sazare, from Oct. '92.

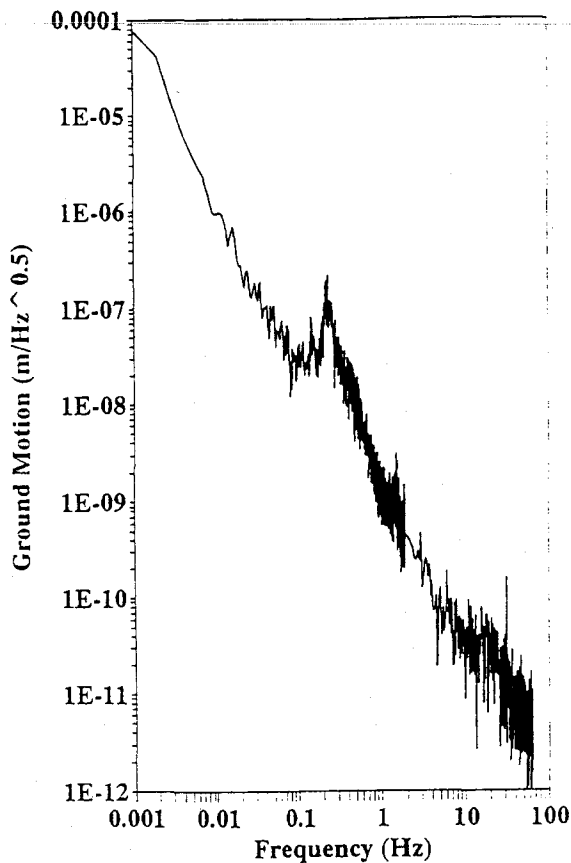


Fig. 9. Spectrum at Sazare.

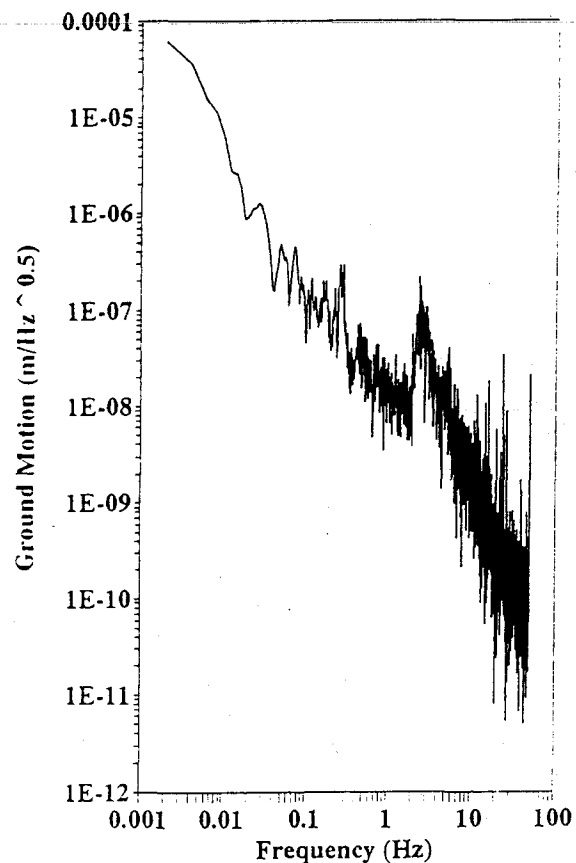


Fig. 10. Spectrum at KEK.

Figures 9 and 10 give power spectra observed by the seismometer at Sazare and at the KEK tunnel, respectively. These spectra are used in the next chapter to extrapolate the empirical frequency law to high frequency. Comparing both figures, the following are features. There is no sharp peak in Fig. 9, except a broad peak around 0.2 Hz, as contrasted with many sharp peaks are there in Fig. 10. It seems that these sharp peaks correspond to the mechanical vibration induced by the cooling water system and/or the traffic activity etc.. The broad-bump about 2 to 4 Hz also corresponds to the human activity. A broad peak about 0.2 Hz is usually explained by the effect of ocean swell with a meteorological influence [12]. The vibration level of the KEK tunnel is, even if we exclude those peaks, considerably high in comparison with that of Sazare, and it becomes more than a factor of ten, at the frequency range from 0.5 to 50 Hz.

4. OVERVIEW OF GROUND MOTIONS

In this chapter, we will try to get an empirical spectrum law of ground movement for wide frequency range, from 1nHz to 100Hz. It is useful for future accelerator design to guess the tolerance of the machine. Figure 11 shows several straight lines. These lines were obtained from many data as excluding sharp peaks and/or broad peaks from the observed spectrum. Typical references are shown in Fig. 11. Two points showed E13 and E1 in Fig. 11 are obtained from the results of crustal movements at Esashi [13]. The point E13 and E1 correspond to drifts of 13 years and one year, respectively.

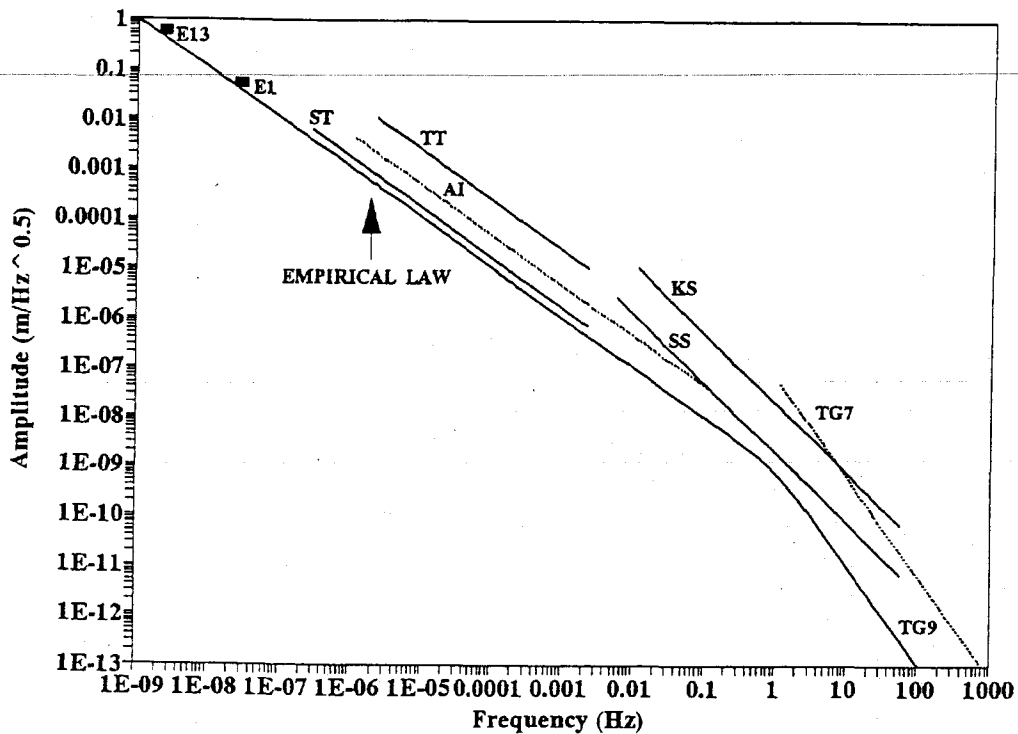


Fig. 11. An empirical spectrum law of ground motion. E13 and E1 ref. [13]: ST is present data by tiltmeter at Sazare: TT is data by tiltmeter at KEK: AI is data by interferometer at outskirts of Tokyo [14]: KS and SS are present data at KEK and Sazare by seismometer: TG7 and TG9 ref. [2].

A simple and empirical power law form of the ground-noise spectrum, except sharp peaks and/or broad peaks from the observed spectrum, can be given as,

$$P(f) \approx kf^{-1}(1+f^2)^{-1/2},$$

where $P(f)$ is a power spectrum in $m/\sqrt{\text{Hz}}$, k is constant and f is frequency in Hz. The factor k is $10^{-9} m/\sqrt{\text{Hz}}$ in a quiet site and $1.5 \times 10^{-8} m/\sqrt{\text{Hz}}$ in a noisy and bad crustal sites. In the actual accelerator tunnel, the power spectrum must be superimposed with the noises of various sorts, such as the activity noises, ocean swell and meteorological noises in every related frequency-band.

5. CONCLUSIONS

The spectrum of crustal movement, can be roughly characterized by $10^{-9} \times (1\text{Hz}/f) m/\sqrt{\text{Hz}}$ between 10^{-9} Hz and 10^{-3} Hz. This proportional coefficient changes with site dependence from $10^{-9} m/\sqrt{\text{Hz}}$ to $1.5 \times 10^{-8} m/\sqrt{\text{Hz}}$. The ground-noise spectrum in the frequency range of 10^{-2} Hz to 100 Hz is very complex. It is, while neither stationary nor smooth, roughly expressed by $1.9 \times 10^{-9} \times (1\text{Hz}/f)^{1.4} m/\sqrt{\text{Hz}}$ on the quiet site. The proportional coefficient on the noisy site is multiplied by a factor of 10-50. In the actual accelerator tunnel, the power spectrum is superimposed with the noises of various sorts as followings;

- (1) vibration induced by cooling system,
- (2) ambient temperature change,
- (3) ocean swell around 0.2Hz,
- (4) noises of human activity in the frequency range 1 to 100 Hz,
- (5) crustal resonance around 3 Hz.

The signals from the interior of the earth such as those of tidal deformations or those of crustal deformations due to tectonic movements are superimposed with the noises of various sorts. There are many varieties in environmental conditions surrounding the tunnel of the accelerator. Differences in geological, geophysical and topographical properties may cause block movement in some case and may change the amplitudes [15]. On the submicron-level alignment of the large scale accelerator, these slow and incoherent drifts can become fatal effects of local conditions. However, we have little information about block crustal movements. Inhomogeneous structure of the earth plays an important role in the ground motion process, which is a rapid stress relaxation by fracturing and the seismic wave scattering. Direct precise measurements of the inhomogeneities are important. We have a plan to observe the space distribution of the ground motion using multiple tiltmeters and broadband seismometers.

ACKNOWLEDGEMENT

The authors sincerely thank Prof. H. Ishii, Earthquake Research Institute, Tokyo University for his useful advice and suggestions. Part of this work was supported by Sumitomo Metal Mining Co., Ltd. and the Nuclear Power Division, Shimizu Corporation. And one of the authors S. T., also thanks Prof. Y. Tamura, National Astronomical Observatory for his cooperative suggestions about the use of BAYTAP-G.

REFERENCES

- [1] T. Aniel and J. L. Laclare, Saclay Report LNS/086 (1985);
J. Roszbach, Part. Acc. Vol. 23, No 2 (1988);
W. Chou, Proc. Part. Acc. Conf. Vol. 2, 906 (1989);
B. Baklakov et al., INP-PREPRINT-91-15;
Y. Ogawa et al., KEK Preprint 92-104, (1992);
V. Shiltsev et al., Proceedings of Emitance-93, in print.
- [2] Technical Report about the Detection of Gravitational Waves,
ed. by N. Mio and M. Oohashi, (in Japanese).
- [3] H. Koiso, S. Kamada and N. Yamamoto, Part. Acc., Vol. 27, 317 (1990).
- [4] S. Takeda, N. Nakanishi, K. Kudo and A. Akiyama, KEK Preprint 92-67,
Int. J. Mod. Phys. A (Proc. Suppl.) 2A (1993), 406.
- [5] JLC Group, JLC-I, KEK Report 92-16 (1992).
- [6] N. Yamamoto, K. Hirata and K. Oide, KEK Preprint 93-20, submitted to the
1993 Particle Accelerator Conference, Washington, D. C., U. S. A.
- [7] H. Ishii et al., Bull. Earthq. Res. Inst. Vol. 67, 79 (1992).
- [8] M. Ishiguro et al., Proc. 9th Int. Sympo., New York, (1981).
- [9] Y. Tamura et al., Geophys. J. Int., Vol. 104, 507 (1991).
- [10] H. Akaike, "Bayesian Statistics", pp. 143-166,
eds. J. M. Bernardo et al., Univ. Press, Valencia, (1980).
- [11] R. Shichi and Y. Okada, J. Geod. Soc. Japan vol 25, 101 (1979).
- [12] G. E. Fisher, SLAC-PUB-3392 (1985).
- [13] Rep. Coordinat. Commit. Earthq. Predict., Vol. 48, (1992).
- [14] K. Asakawa, Doctoral Thesis, (1979).
- [15] M. Yanagisawa, Bull. Earthq. Res. Inst., Univ. Tokyo,
Vol. 65, 161 (1990), (in Japanese).